

Comparison between SAGE II and ISCCP high-level clouds

1. Global and zonal mean cloud amounts

Xiaohan Liao¹

Science Systems and Applications, Inc., NASA Goddard Institute for Space Studies, New York

William B. Rossow and David Rind

NASA Goddard Institute for Space Studies, New York

Abstract. Global high-level clouds identified in Stratospheric Aerosol and Gas Experiment II (SAGE II) occultation measurements for January and July in the period 1985 to 1990 are compared with near-nadir-looking observations from the International Satellite Cloud Climatology Project (ISCCP). Global and zonal mean high-level cloud amounts from the two data sets agree very well, if clouds with layer extinction coefficients of $<0.008 \text{ km}^{-1}$ at $1.02 \text{ }\mu\text{m}$ wavelength are removed from the SAGE II results and all detected clouds are interpreted to have an average horizontal size of about 75 km along the 200 km transmission path length of the SAGE II observations. The SAGE II results are much more sensitive to variations of assumed cloud size than to variations of detection threshold. The geographical distribution of cloud fraction shows good agreement, but systematic regional differences also indicate that the average cloud size varies somewhat among different climate regimes. The more sensitive SAGE II results show that about one third of all high-level clouds are missed by ISCCP but that these clouds have very low optical thicknesses (<0.1 at $0.6 \text{ }\mu\text{m}$ wavelength). SAGE II sampling error in monthly zonal cloud fraction is shown to produce no bias, to be less than the intraseasonal natural variability, but to be comparable with the natural variability at longer time scales.

1. Introduction

Clouds with tops higher than the effective emission-to-space level of the clear atmosphere affect the radiation balance differently than lower level clouds. While the latter primarily reduce the shortwave (0.2 to $5.0 \text{ }\mu\text{m}$ wavelengths) radiative heating of the surface, higher-level clouds shift the direct solar heating of the atmosphere to higher altitudes and decrease longwave (5.0 to $200.0 \text{ }\mu\text{m}$ wavelengths) radiative cooling of the atmosphere. Simulations with general circulation models have shown that changes in high-level clouds affect the surface climate by altering the atmospheric circulation [Randall *et al.*, 1989; Slingo and Slingo, 1988; Ramaswamy and Ramanathan, 1989]. The net radiative effect of high-level clouds depends on their optical thickness: Thinner clouds produce little change of shortwave heating but increase longwave heating at their base, whereas thicker clouds also increase shortwave heating in the upper atmosphere at the expense of the surface. Satellite observations have been regarded as the primary way to investigate the large-scale variations in high-level cloud properties, but the low optical thicknesses of many high-level clouds and confusion with lower-level clouds in most satellite views have made reliable and top locations is obtained for the topmost cloud layer from the infrared emission [Rossow and Schiffer, 1991]. This radiometric cloud top

complete surveys difficult. We may learn more about high-level clouds, particularly the optically thin ones, by comparing and combining results from completely different satellite observing techniques.

Since 1984 the Stratospheric Aerosol and Gas Experiment (SAGE II) [McCormick *et al.*, 1976, 1979], aboard the Earth Radiation Budget Satellite (ERBS), has monitored aerosols, ozone, water vapor, and NO_2 in the upper troposphere and stratosphere, using a limb occultation technique. Because the SAGE II instrument directly views the Sun before and after viewing it through the atmosphere over a path length of about 200 km, the measurements are very sensitive to the presence of particle scattering and are not confused by any background source of radiation. By looking for extinction of solar radiance at $1.02 \text{ }\mu\text{m}$ wavelength greater than that predicted for a gas atmosphere in a field of view of about 0.5 km, the measurements directly indicate the location of the physical cloud top with relatively high vertical resolution. However, the long atmospheric path length also means that even relatively optically thin clouds can completely block any detectable radiation from the Sun. Hence thin upper level clouds block detection of lower level clouds. Moreover, the horizontal coverage by clouds along this long path is uncertain.

Since 1983 the International Satellite Cloud Climatology Project (ISCCP) [Schiffer and Rossow, 1983] has collected and analyzed infrared ($\approx 11 \text{ }\mu\text{m}$) and visible ($\approx 0.6 \text{ }\mu\text{m}$) radiances measured by the imaging radiometers on operational weather satellites that view the Earth in a direction near their nadir. The ISCCP results provide a detailed description of the horizontal variations of cloud top pressure and optical thickness (approximately 5 km image pixels are sampled at a spacing of about 30 km), where the ISCCP estimate of cloud

¹Formerly at Hughes STX Corporation, New York.

will coincide with the physical cloud top if the cloud optical thickness is greater than about 4 and concentrated in a physically thin layer. Location of optically thin clouds is difficult because of confusion with surface temperature variations (detection sensitivity) or, since the ISCCP analysis treats all scenes as containing a single cloud layer, because thinner high-level clouds overlying thicker low-level clouds may not be recognized as high-level.

If the frequencies of occurrence of high-level clouds from Woodbury and McCormick [1986] are interpreted to be cloud amounts, then their average value is about 2 to 3 times as large as the horizontal cloud fractions determined from nadir-viewing satellite observations [Barton, 1983]. A similar result holds for the comparison with ISCCP cloud amounts. Woodbury and McCormick pointed out, however, that the frequency of SAGE II cloudy events would match the traditional cloud cover fraction only when all clouds observed occupy the entire horizontal view of SAGE II. We show that if we determine the frequency of occurrence of high-level clouds from ISCCP, it is nearly the same as that determined from SAGE II.

Since we have access to the individual SAGE II and ISCCP measurements, instead of being limited to average results, a more detailed comparison of these two data sets can help answer the following questions.

1. Since SAGE II has much sparser and more irregular sampling of clouds than ISCCP, does this sampling affect the mean cloud properties deduced from SAGE II measurements?

2. Since the SAGE II radiance measurements are more sensitive to the presence of optically thin clouds than ISCCP measurements, by how much does this difference in detection sensitivity affect the amount of high-level cloud determined with the two techniques?

3. Since SAGE II measures cloud top location more directly than ISCCP, what is the difference in ISCCP radiometric cloud top pressures, and by how much does this difference in cloud top locations affect the amount of high-level cloud determined with the two techniques?

4. Since the horizontal resolution of ISCCP cloud detection is much higher than that for SAGE II, by how much does this difference in resolution affect the determination of high-level cloud amounts?

To investigate these questions, we have compared SAGE II and ISCCP high-level cloud amounts for all Januarys and July from 1985 through 1990. Detailed descriptions of the data sets, their viewing geometries, and the matching procedure are given in section 2. In this paper we discuss all four questions above by comparison of identifications of high-level clouds and of determinations of their amounts (section 3). In a companion paper [Liao *et al.*, this issue] we further compare the cloud top pressures inferred from matched individual SAGE II and ISCCP observations of high-level clouds and investigate how the structure of the upper portions of the clouds affects the determination of cloud top location. Section 4 summarizes the uncertainties in high-level cloud amounts while, section 5 discusses other key conclusions.

It needs to be noted that we are comparing two instruments that have different levels of sensitivity and that may not be seeing clouds at the same level or of the same horizontal extent. Section 3 shows that the straight use of SAGE II cloud threshold produces much larger cloud amount than ISCCP. As shown in section 3, the sensitivity differences between these two data sets are reduced by tuning the cloud threshold of SAGE II to agree with ISCCP. Also, the introduction of cloud horizontal size with SAGE II cloud data helps to eliminate the differences in the horizontal extent on a climatological basis. In addition, because the comparison here only discusses the highest level of SAGE II clouds (except an optically thin cirrus overlapping a thick cloud), this also reduces the chance of mismatch between ISCCP and SAGE II cloud top altitudes.

2. Data Sets and Analysis Methods

2.1. SAGE II and ISCCP: The Way They Look at Clouds

The SAGE II instrument views the Sun at seven wavelengths as it rises or sets behind Earth's limb (Figure 1). Vertical profiles of the extinction by the atmosphere at $1.02 \mu\text{m}$ wavelength are used to detect aerosols and clouds, because this wavelength is not sensitive to variations of trace gas species [Woodbury and McCormick, 1986; Chu *et al.*, 1993]. Aerosol and clouds can be separated by using two wavelengths to discriminate particle size differences [Kent *et al.*, 1993]. About 30 locations at two latitudes are observed per day; as the satellite orbit plane precesses, coverage from about 79°S to 79°N is accumulated after a few months, although the frequency of observations diminishes at latitudes poleward of 55° . Since there are only about 900 SAGE II observations per month, we match individual SAGE II and ISCCP observations in all six Januarys and July from 1985 to 1990.

A single atmospheric profile is taken from a height (line of sight tangent to the surface) of 150 km, where there is no atmospheric attenuation, down to complete loss of signal, where the line of sight encounters either a thick cloud or the surface. The height where a SAGE II profile ends is called the saturated height. Statistics on the frequency of penetration to various levels are given by Rind [1993]. The field of view of the $1.02 \mu\text{m}$ channel perpendicular to the line of sight is 0.5×2.5 arc min, which corresponds to a vertical dimension of about 0.5 km in the atmosphere. The horizontal path in the atmosphere is about 200 km in length. More details are given by McCormick *et al.* [1979] and Rind *et al.* [1993].

Radiance observations at $1.02 \mu\text{m}$ are compared with the predicted extinction of a gaseous atmosphere to obtain aerosol and/or cloud extinction coefficients, $k(h)$, for every 1-km-thick layer (assuming a path length of 200 km) from the lower mesosphere down into the lower troposphere [Chu and McCormick, 1979; Chu *et al.*, 1993]. Note that each lower level is viewed through all the layers above, so that the extinction coefficient at each level is the difference between the measured total value and the sum of values in all upper levels. Single-layer values of extinction coefficient in excess of 0.0008 km^{-1} are taken to indicate the presence of cloud along the 200 km path length at that altitude [Woodbury and McCormick, 1986]; this extinction is a few times larger than the normal background aerosol extinction coefficient [Kent *et al.*, 1993]. The first occurrence of excessive extinction defines cloud top location. A sudden cutoff of signal in a profile before reaching the surface implies that a relatively thick cloud has been encountered. Thus the statistic measured by SAGE II is the cloud frequency of

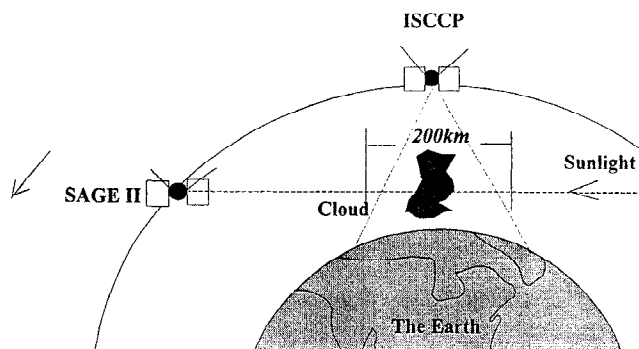


Figure 1. Schematic illustration of SAGE II and ISCCP cloud observation geometry. The horizontal domain over which ISCCP determines cloud fraction is ≈ 280 km in size. The path length of SAGE II observations is ≈ 200 km.

occurrence; to determine cloud amount, this quantity must be multiplied by the amount of cloud when present [Woodbury and McCormick, 1986].

All ISCCP cloud observations are collected from near-nadir-looking satellite instruments (Figure 1). Global coverage is provided by a combination of up to five geostationary satellites and up to two polar orbiting satellites. Individual image pixels (about 4–7 km across) are classified as clear or cloudy depending on whether either the infrared ($\approx 11 \mu\text{m}$) or visible ($\approx 0.6 \mu\text{m}$) radiance differs from the inferred clear scene value by more than some threshold amount, where the clear sky radiances at these wavelengths depend primarily on the characteristics of the surface. The thresholds represent the estimated uncertainty of the clear radiance values; thus the detection sensitivity of the ISCCP results is limited by how accurately the clear radiances can be determined, which in turn is determined by how variable the clear radiances are. For ISCCP, infrared radiances are given as brightness temperatures, whereas visible radiances are given as a percentage of the instrument's measurement when viewing a surface with a Lambertian reflectivity of unity. The infrared and visible thresholds are, respectively, 2.5 K and 3% over oceans and 6 K and 6% over land. More details are documented by Rossow and Garder [1993a], (see also Rossow *et al.* [1991]). The sensitivity of detecting optically thin, high-level clouds is estimated to be equivalent to a lower limit on the visible ($\approx 0.6 \mu\text{m}$ wavelength) optical thicknesses of 0.1–0.3, depending on cloud top altitude [Wielicki and Parker, 1992; Rossow and Garder, 1993b].

In the ISCCP analysis, a cloud cover of either 0 or 1 is assigned to individual image pixels that are spatially sampled at an interval of about 30 km. Cloud amounts are determined for regions that are about 280 km across by counting the fraction of the total number of image pixels that are cloudy in the region. Although there are sampling effects, the statistical spatial resolution is equivalent to the pixel size [Seze and Rossow, 1991; Rossow *et al.*, 1993], and the cloud amount for the 280 km region does represent fractional area coverage [Rossow *et al.*, 1993]. The cloud top temperature (and pressure) is retrieved from the infrared radiance and the cloud optical thickness is retrieved from the visible radiance [Rossow *et al.*, 1991]. For optically thick clouds with distinct (sharp) top boundaries, the infrared radiation originates from very near the physical top of the cloud, so that the cloud top pressure of such clouds is well determined. For clouds with very diffuse upper boundaries, the radiation originates deeper in the cloud, and the top pressure will be overestimated. For higher-level optically thin clouds, radiation from below makes the cloud temperature appear larger. However, this effect can be accounted for if the observed visible reflectance represents the optical thickness of the whole cloud layer, as it does when a higher-level cloud occurs alone. When another cloud layer occurs below, then the sum of the two optical thicknesses is attributed to the upper layer in the ISCCP analysis, and the cloud top temperature (pressure) will also be overestimated.

2.2. SAGE II Extinction Coefficient at 1.02 μm and ISCCP Vertical Optical Thickness at 0.6 μm

The primary SAGE II observations are interpreted in terms of an extinction coefficient at 1.02 μm wavelength, $k_i(1.02 \mu\text{m})$ for each atmospheric level. Calculation of the $k_i(1.02 \mu\text{m})$ is illustrated by Chu and McCormick [1979]. Generally speaking, the k_i is determined from the total horizontal attenuation of the sunlight intensity at the tangent height for layer i and the attenuation in the layers above.

The vertical optical thickness τ of SAGE II clouds can be approximated by the vertical extent of the cloud layer, ΔZ , multiplying an average cloud extinction coefficient k_{ic} over N cloudy layers. As we show below, the average horizontal path length in cloud appears to be about 75 km, instead of the 200 km value used in the SAGE II analysis. Thus

$$k_{ic} \approx \frac{200 \text{ (km)}}{75 \text{ (km)}} \left(\frac{1}{N} \sum_1^N k_i \right) \quad (1)$$

The ISCCP observations are given in terms of total column optical thicknesses τ at 0.6 μm wavelength determined from the observed visible reflectivity. Cloud particles are generally much larger than these two wavelengths (1.02 and 0.6 μm), so that the wavelength dependence of extinction (mostly scattering) is very weak. Based on Mie scattering calculations with spherical ice, $k_{ic}(1.02 \mu\text{m}) \approx k_{ic}(0.52 \mu\text{m})$, as confirmed by SAGE II observations [Kent *et al.*, 1993]. Hence as a useful approximation (none of our results depends on this estimate),

$$\tau \approx k_{ic} \times \Delta Z \quad (2)$$

Since $k_{ic}(1.02 \mu\text{m}) \approx k_{ic}(0.52 \mu\text{m})$, we will use τ, k_i in the following sections without indicating wavelength; however, the wavelengths at which they are measured are to be understood.

The sensitivity of the SAGE II instrument limits Σk_i to about 0.08. According to equations 1 and 2, a complete extinction profile from SAGE II that is not saturated corresponds to optical thickness less than 0.2, if $\Delta Z=2.5 \text{ km}$ (see later sections). For saturated profiles, k_i for the saturated layer is unknown, but probably greater than 0.03 km^{-1} . The maximum layer extinction coefficient is about 0.04 km^{-1} (W. P. Chu, personal communication, 1994), when averaged over the saturated layer and all layers with higher tangent altitudes. In cases where higher cloudy layers exist so as to contribute to the cutoff extinction, their contribution is typically less than 0.01 km^{-1} . So treating the extinction coefficient at the saturated layer as greater than 0.03 km^{-1} is pretty conservative in the upper troposphere except after the eruption of a sizable volcano. A survey of the whole SAGE II data set for January and July showed the maximum value of k_i to be 0.027 km^{-1} , consistent with this estimate. Thus as long as the threshold value of k_i used to detect clouds in the SAGE II data is $<0.03 \text{ km}^{-1}$, we may treat all saturated profiles as cloudy. For rough estimation, using equations 1 and 2, if the typical cloud thickness is about 2.5 km, then a saturated extinction, 0.03–0.04, corresponds to an optical thickness of SAGE II cloud in a saturated profile than is most likely larger than 0.3.

2.3. Matching Times and Locations of SAGE II and ISCCP Observations

The ISCCP data set (stage C1) represents the global, merged results from four to six satellites reporting every 3 hours at a spatial resolution of about 280 km. SAGE II has rather irregular sampling with time intervals at one location ranging from about 1 hour to a few days. In any particular month the irregularly distributed observations by SAGE II do not sample some large regions at all. Therefore the first step in this comparison is to match each observation in the entire SAGE II data set to an ISCCP C1 observation at the corresponding location and time to reduce differences associated with the different sampling of the two data sets. Only about 8% of the SAGE II data set has no corresponding ISCCP observation, mostly at the highest latitudes. Because the ISCCP cloud analysis is less reliable in polar regions [Rossow and Garder, 1993b] and the SAGE II sampling is so sparse there, we limit our study to $\pm 55^\circ$ latitude.

A single ISCCP map grid cell is an equal area cell equivalent to $2.5^\circ \times 2.5^\circ$ ($280 \text{ km} \times 280 \text{ km}$) at the equator. A single SAGE II sample represents a horizontal domain about $200 \text{ km} \times 0.5 \text{ km}$ (SAGE II location errors are estimated to be $<100 \text{ km}$, [Jones, 1992]), about 0.1% of the area of the ISCCP grid cell. The ISCCP data set represents a distributed sample of this same area that covers from 0.6% to almost 5% of the total area. Therefore we must expect differences between individual SAGE II and ISCCP estimates of cloud amount because of these differences in spatial sampling [cf. Rossow et al., 1993].

SAGE II measurements occur only at sunrise and sunset. Since the daytime observations of ISCCP can be interpreted more completely by using the visible channel [Rossow and Schiffer, 1991], we use only daytime ISCCP results. For any pair of SAGE II and ISCCP observations, the time difference is constrained to be <9 hours to maximize the number of samples; most matches have time differences of <6 hours. Jones [1992] reported that cloud cover observations are highly correlated over time differences of 6-9 hours; however, some differences between individual observations will occur because of these differences in temporal sampling.

The matched data sets provide about 9000 total observations from the combination of six Januaries and six Julys. Figure 2 illustrates the locations covered by joint observations for all Julys. Unless otherwise indicated, all investigations below are based on the matched data sets. Of these 9000 observations, roughly 1600 (18% of the total) are clear of high-level clouds according to both SAGE II and ISCCP. Henceforth all fractional populations of the observations will be reported in percent, whereas cloud amounts will be reported as fractions from 0 to 1. In another 1400 cases (16%), ISCCP indicates some cloudiness, but SAGE II does not; in 1350 cases (15%), SAGE II indicates clouds, but ISCCP does not (see section 3.1). In the remaining 4600 cases, both data sets indicate the presence of clouds.

In the SAGE II analysis, we follow Woodbury and McCormick [1986] by defining the highest level where $k_i > K$, the threshold value, as the cloud top altitude, h_i . Consecutive layer extinction coefficients above the threshold on the same profile are regarded as one cloud event. They defined a "high" cloud by a top in the height range, $ZT + 2 \text{ km} \geq h_i \geq 0.7 ZT$ or 8 km , whichever is larger (ZT is the height of tropopause). In the ISCCP analysis, cloud top pressure is determined from the retrieved cloud top temperature compared with an atmospheric temperature profile [Rossow et al., 1991]; all cloud tops at pressures of $<440 \text{ mbar}$ are identified as high-level clouds. For a more precise comparison between SAGE II and ISCCP results, high-level SAGE II clouds are redefined by cloud top pressures $<440 \text{ mbar}$. Woodbury and McCormick [1986] also

divided high clouds into "thin cirrus" and "cirrus" by extinction coefficients less than or greater than 0.008 km^{-1} , whereas in the ISCCP analysis, high clouds are subdivided into three optical thickness ranges [Rossow and Schiffer, 1991]. For our comparisons in this paper we retain only a single high-level cloud category (cloud top pressure of $<440 \text{ mbar}$) for both data sets, except where otherwise stated.

3. High-Level Cloud Amount Comparisons

Figure 3 shows the zonal mean SAGE II high-level cloud frequencies of occurrence (using $K = 0.0008 \text{ km}^{-1}$), individually matched to ISCCP observations, and the zonal mean ISCCP high-level cloud amounts, both averaged over all Julys and Januaries in 1985 through 1990. As in previous comparisons of limb-viewing and nadir-viewing satellite results, the frequency of high-level clouds from SAGE II is about 3 times the cloud amount from ISCCP with little

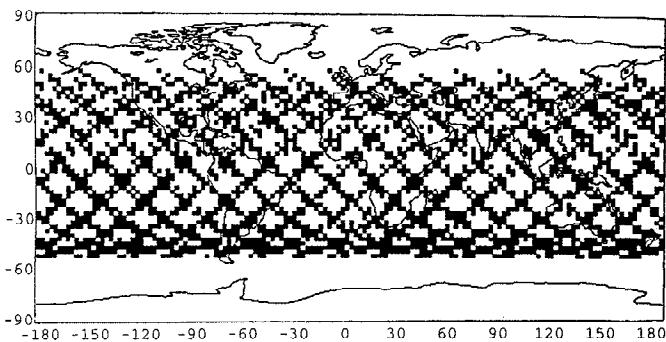
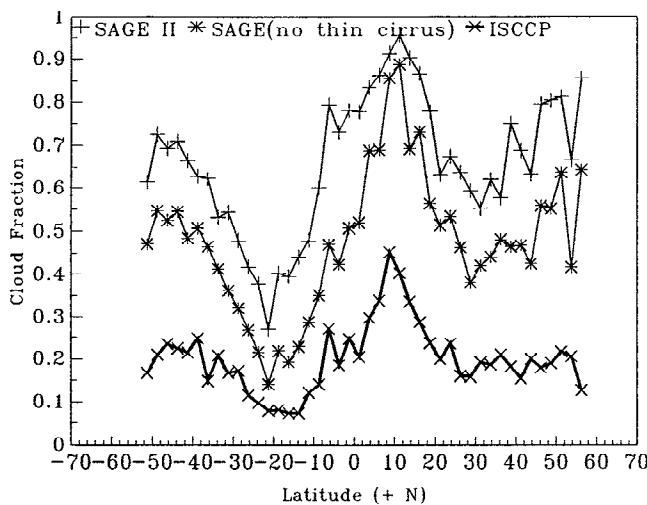
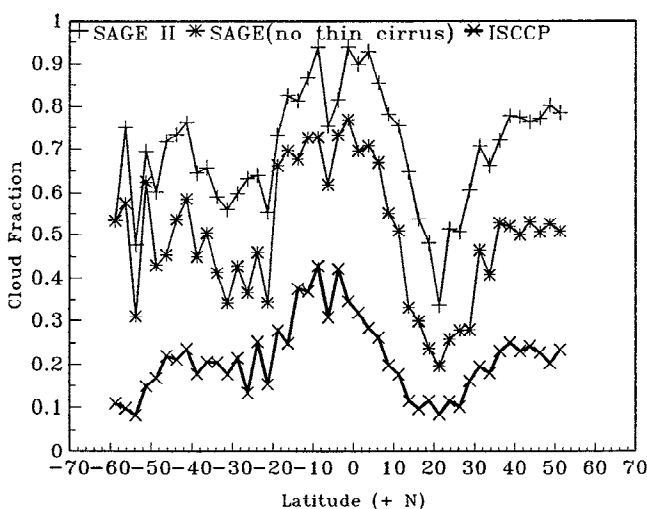


Figure 2. Global coverage by SAGE II for July 1985-1990. Each black square represents those $2.5^\circ \times 2.5^\circ$ regions in which SAGE II observations occurred.



(a)



(b)

Figure 3. Zonal mean high-level cloud amounts for (a) July 1985-1990 and (b) January 1985-1990 from SAGE II using a threshold extinction coefficient $K = 0.0008 \text{ km}^{-1}$ (line with pluses), using a threshold $K = 0.008 \text{ km}^{-1}$ (line with asterisks), and from ISCCP (thick line with crosses).

seasonal variation. Even with the “thin cirrus” category removed from the SAGE II results (by using $K > 0.008 \text{ km}^{-1}$), they still are about double the ISCCP values. Despite this large systematic difference, both data sets show the same large-scale relative variations with latitude, revealing the stormy tropical and midlatitude zones and the seasonal change in the position of the Intertropical Convergence Zone (ITCZ). The correlation between the zonal mean curves is high, 0.88 (99.99% confidence level) for July and 0.82 (99.99% confidence level) for January.

The systematic difference can be explained by four possible causes.

1. The detection sensitivity of ISCCP is less than that of SAGE II, causing an underestimate of high-level cloud amounts. SAGE II measures solar extinction along a 200 km path through Earth’s atmosphere (Figure 1) and needs only an integrated horizontal optical thickness of >0.16 to exceed the background aerosol and gas extinction [Kent *et al.*, 1993], which is equivalent to an extinction coefficient of 0.0008 km^{-1} if the cloud occupies the whole 200 km path. Because the satellite radiometers used for ISCCP look almost vertically downward toward Earth’s surface, a cloud needs a moderate vertical optical thickness to change the measured radiances by more than the uncertainty in the clear sky values, which are determined primarily by surface properties. For high clouds over oceans, the estimated detection limit for ISCCP is equivalent to a vertical optical thickness of ≈ 0.1 [Wielicki and Parker, 1992]; over land the detection limit is ≈ 0.3 [Rossow and Garder, 1993b]. Using equations (1) and (2), we see that these ISCCP thresholds are roughly equivalent to SAGE II extinction coefficient $0.015\text{--}0.045 \text{ km}^{-1}$ (assuming the cloud layer is 2.5 km and the cloud horizontal size is 75 km in the SAGE II path length of 200 km), which is close to the maximum values observed by SAGE II, except for saturated profiles. This difference in sensitivity would produce cases where SAGE II detects the presence of clouds, but ISCCP does not.

2. Moreover, the ISCCP analysis can only recognize the presence of the thinner high-level clouds when they occur alone because the presence of lower-level clouds results in an overestimate of cloud top pressure. Co-occurrence statistics suggest that this may happen as much as half the time [Warren *et al.*, 1985]. Hence we expect that errors in cloud top pressures will cause the mislabeling of some of the optically thinnest clouds as lower-level clouds, underestimating high-level cloud amounts even more relative to SAGE II. This effect would produce cases where SAGE II detects the presence of high-level clouds, but ISCCP does not.

3. There is a large difference in the ratio of the horizontal resolution of the observations to the average cloud size between SAGE II and ISCCP. The SAGE II analysis cannot estimate what portion of its 200 km path length through the atmosphere is actually occupied by the clouds it detects. If the average cloud size is smaller than 200 km, then determining cloud amount from the SAGE II

detection frequencies, as we do, would overestimate total cloud amount when compared with ISCCP (which reports fractional cloudiness within a 280 km cell). The nadir-looking instruments used by ISCCP have an average resolution of about 5 km. Studies of higher-resolution satellite measurements [Wielicki and Parker, 1992], together with global distributions of cloud amount frequencies at two different spatial resolutions (about 30 km and 280 km), suggest that the average cloud size is much larger than 5 km [Rossow *et al.*, 1993] but smaller than 200 km. Thus we expect that low horizontal resolution may cause the SAGE II analysis to overestimate high-level cloud amounts relative to ISCCP. Note that this effect does not produce a mismatch of detection frequencies.

4. However, since the SAGE II observation samples only about 0.1% of the ISCCP grid cell area, there is finite chance that SAGE II will miss clouds, even though ISCCP reports some to be present, but the area coverage is low. This effect would decrease SAGE II frequencies of occurrence, offsetting the other three effects.

Table 1 shows the detection match-up statistics for two different SAGE II detection thresholds: This table reports only whether either SAGE II or ISCCP sees any cloud at all. First, notice that the ISCCP frequency of occurrence of high-level cloudiness is 67%, roughly the same as the global mean frequency from the matched SAGE II (see Table 2). Moreover, SAGE II and ISCCP agree on the presence of clouds in 69% of the individual cases. Thus the third effect listed above is probably the dominant cause of the cloud amount discrepancy.

Second, notice that the match-up category that would be produced by a mislabeling of high-level clouds as lower-level clouds by ISCCP (category 3 in Table 1) contains only 15% of the cases, and about half of these are very thin clouds that are not detected by ISCCP, as evidenced by the change caused by increasing the SAGE II detection threshold. Thus errors in cloud top pressure that result in a mislabeling of clouds by ISCCP can account for 7% of the cases at most. If these additional cases contribute a similar cloud cover when present as other high-level clouds, then a high bias of cloud top pressure reduces the ISCCP high-level cloud amount by only about 0.02 ($7\% \times 0.21 + 67\%$).

Third, a higher SAGE II detection sensitivity affects about 18% of the cases, increasing categories 3 and 4 in Table 1 when the SAGE II detection threshold is decreased. However, in about half of these cases, ISCCP is already detecting some cloudiness, apparently spatially associated with the thinner clouds detected by SAGE II.

On the other hand, the category that would be produced by missed SAGE II detections because its area sample is so small (category 2 in Table 1) contains 16% of the cases. Evidence that these cases are caused by area sampling is provided in Figure 4, which shows the frequency distribution of ISCCP cloud amounts for cases matched with SAGE II cloud detections (cases where both ISCCP

Table 1. Cloud Detection Match-up Statistics for SAGE II and ISCCP Cloud Observations

Population Category	SAGE	ISCCP	K_{low}	K_{high}
1	clear	clear	18	26
2	clear	cloudy	16	26
3	cloudy	clear	15	7
4	cloudy	cloudy	51	41

The total population of observations from six Januarys and Julys is about 9000; populations in each category are given as a fraction in percent. K is the extinction coefficient threshold, where $K_{low} = 0.0008 \text{ km}^{-1}$ and $K_{high} = 0.008 \text{ km}^{-1}$.

Table 2. Comparison of Global Mean High-Level Cloud Amounts for July and January Averaged Over 1985–1990 From the Matched SAGE II and ISCCP Data Sets

Threshold K , km^{-1}	l , km	SAGE II	
		July	January
0.0008	200	0.690	0.746
0.0080	200	0.465	0.502
Saturated only (≈ 0.025)	200	0.360	0.370
0.0008	75	0.297	0.321
0.0080	75	0.204	0.216
Saturated only (≈ 0.025)	75	0.155	0.159
ISCCP values		0.203	0.218

The same cloud top location range was used. The SAGE II cloud detection sensitivity is determined by the threshold extinction, K . The extinction coefficient for the saturated layer is unknown, but is assumed to be large enough to exceed the threshold extinction. The assumed horizontal dimension of the clouds along the 200 km SAGE II path length is given by the value of l . The optimum values of K and l are determined by the best agreement between global mean and zonal mean SAGE II and ISCCP cloud amounts in July.

and SAGE II detect clouds) and for cases matched with no SAGE II cloud detection (cases where ISCCP detect clouds but SAGE II does not). The generally very low ISCCP cloud amounts in the latter case make it very likely that SAGE II would miss clouds more often. Some portion of this category may also be produced by false cloud detections by ISCCP, especially over winter land areas, but the frequency of these false detections is estimated to be $<5\%$ [Rossow and Garder, 1993a; Rossow et al., 1993].

To clarify further the contributions of detection sensitivity and horizontal resolution to the differences shown in Figure 3, we vary the SAGE II detection threshold and the assumed horizontal cloud dimension, together and separately, to determine the best agreement.

3.1. Effect of Varying Cloud Detection Sensitivity

To explore the first possibility stated in the last section, we calculate SAGE II cloud amounts, using a range of extinction thresholds from 0.0001 to 0.025 km^{-1} . Only the SAGE II obser-

vations matched to ISCCP are used, with high-level cloud defined in the same way as for ISCCP. As expected, the significantly larger SAGE II cloud amounts as compared with ISCCP (Figure 3) are reduced by increasing the detection threshold, but it turns out that even at the highest available extinction threshold, about 0.025 km^{-1} , we still have a SAGE II cloud frequency of occurrence about twice the ISCCP value (Table 2), and the root-mean-square difference between their zonal monthly mean values is still as high as 0.2. For extinction thresholds higher than 0.025 km^{-1} , the only SAGE II clouds are saturated profiles.

This result indicates that a simple increase of the SAGE II extinction thresholds does not produce a good match of SAGE II and ISCCP. Even if some clouds with saturated profiles have vertical optical thicknesses less than the ISCCP detection limit, removal of such clouds does not improve the overall match between SAGE II and ISCCP.

3.2. Effect of Varying Cloud Horizontal Size

Cloud fraction is defined as the portion of the horizontal area occupied by cloud. In the ISCCP analysis, cloud fraction is defined over an area as the percentage of the total number of image pixels (in the sampled collection) that are found to contain clouds. Since the sampled pixels are statistically similar to the total population [Seze and Rossow, 1991], the effective resolution of the cloud fraction measurement is the pixel size, about 5 km.

For SAGE II, monthly mean cloud frequency of occurrence for each grid cell is given by the ratio of the number of cloudy events to the total number of observations. Although SAGE II can detect a cloud somewhere along the 200 km path in the atmosphere, it cannot determine how much of the path length is occupied by clouds. For example, if the cloud horizontal size is only 50 km, then a nadir-looking observation would conclude that the cloud fraction along the 200 km path is $50/200 = 0.25$. If we assume that cloud variations are horizontally isotropic, then the two-dimensional cloud cover could be 0.0625 in this case. The actual situation will be much more complicated, since small clouds tend to occur in larger-scale fields with separation distances that are only a few times larger than the element sizes [Welch et al., 1988; Cahalan and Joseph, 1989; Dowling and Radke, 1990]. Thus as the average size of the cloud

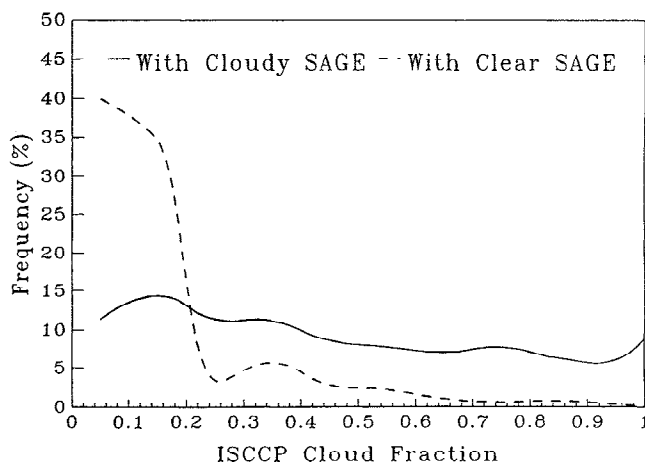


Figure 4. Distribution of ISCCP cloud fractions for matched observations where both SAGE II and ISCCP report clouds (solid line) and for matched observations where SAGE II does not report clouds (dashed line), using $K = 0.008 \text{ km}^{-1}$.

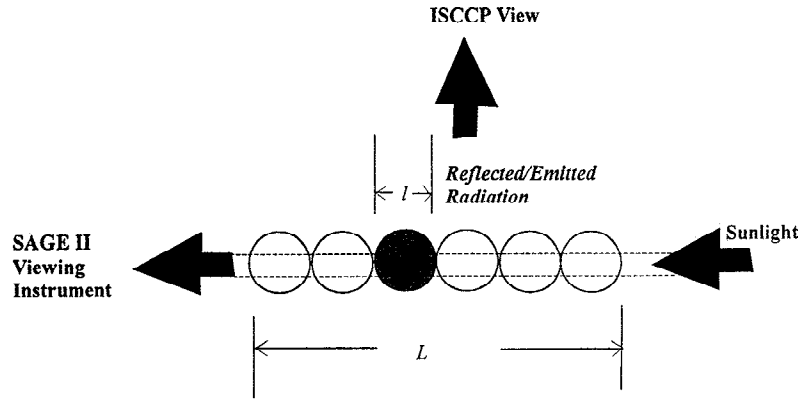


Figure 5. Schematic of one-dimensional representation of SAGE II and ISCCP view of clouds where each cloud element has a size of l km along the SAGE II path length $L=200$ km. Each circle represents one element, and shaded circles represent a cloudy element.

elements decreases, the number of clouds along a 200 km path is likely to increase. Since we treat all SAGE II cloud observations as completely cloud covered for each ISCCP grid cell (e.g. in Figure 3), a smaller average cloud element size, even with multiple occurrences along the path length, will reduce cloud amounts. Rossow *et al.* [1993] show that the cloud amount frequency distribution for the ISCCP grid resolution indicates only about 60% of the cases with cloud fractions of 0 or 1.

As one simple estimate of the magnitude of this effect, we consider the one-dimensional problem illustrated in Figure 5. We assume that all clouds have the same size, represented by the dimension l . We use the higher-resolution ISCCP global average cloud fraction, F , to represent the frequency of occurrence of such clouds along each 200 km path length and assume that this accounts approximately for the complexities of multiple cloud elements being present when clouds are broken. Thus the probability of a single element being clear is

$$p_{clr} = 1 - F \quad (3)$$

and the probability of the whole path being clear is

$$P_{clr} = p_{clr}^{200/l} = (1 - F)^{200/l} \quad (4)$$

where we assume that the number of independent samples of size l along a 200 km path length is $200/l$. The probability of a cloudy event observed by SAGE II is then

$$P_{cld} = 1 - (1 - F)^{200/l} \quad (5)$$

The value of p_{cld} is the SAGE II frequency of occurrence when the cloud fraction is F . To convert other SAGE II frequencies of occurrence, f_{SAGE} , to cloud fractions, f_c , for an assumed value of l , we use

$$f_c = \frac{F}{P_{cld}} \times f_{SAGE} \quad (6)$$

Since the actual situation involves broad cloud size distributions and complex spacing of the smaller clouds, the value l should be considered to be only an effective size that is an average over all the size and separation distributions of clouds.

Figure 6 shows the values of (F/P_{cld}) as a function of the assumed cloud size, l . As $l \rightarrow 0$, the number of samples goes to infinity and $P_{cld} \rightarrow 1$, and SAGE II cloud fraction is given by $F * f_{SAGE}$. In practice, this limit is reached when $l < 10$ km. When the cloud is as large as the path length, $l = 200$ km, then the cloud fraction equals

the frequency of occurrence, f_{SAGE} . For values of l between 10 and 200 km, the SAGE II cloud fraction varies linearly from about 0.14 to 0.07 (see Table 2).

3.3. Effect of Varying Both Cloud Detection Sensitivity and Horizontal Size

To find the best match between SAGE II and ISCCP cloud fractions in terms of the correlation between their latitudinal variations and the minimum rms differences, the SAGE II values are recalculated with horizontal cloud sizes, l , in the range 30 km to 125 km. For each l we also find the extinction threshold, K , at which the globally averaged SAGE II cloud fraction equals the ISCCP value. Because the SAGE II cloud frequency is almost twice the ISCCP cloud fraction, even if we choose the highest extinction coefficient available in SAGE II, we would still need almost a 50% reduction ($l = 125$ km) in the SAGE II cloud size to match ISCCP values. We evaluate the agreement between SAGE II and ISCCP by comparing the zonal mean cloud fractions averaged over all Julys. Figure 7a shows that the combinations of cloud horizontal sizes

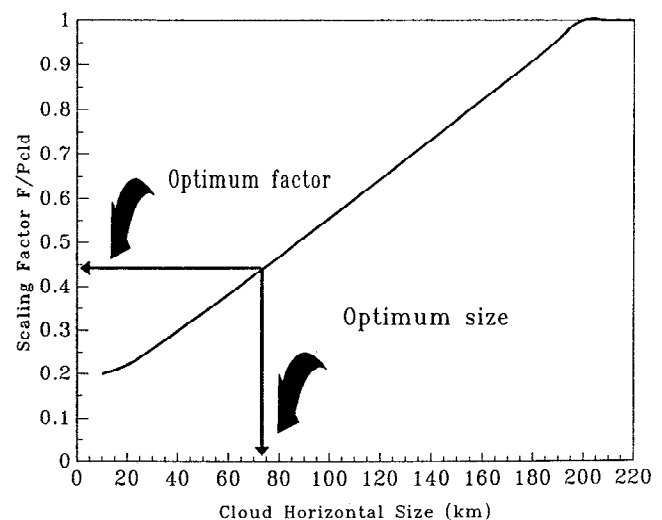
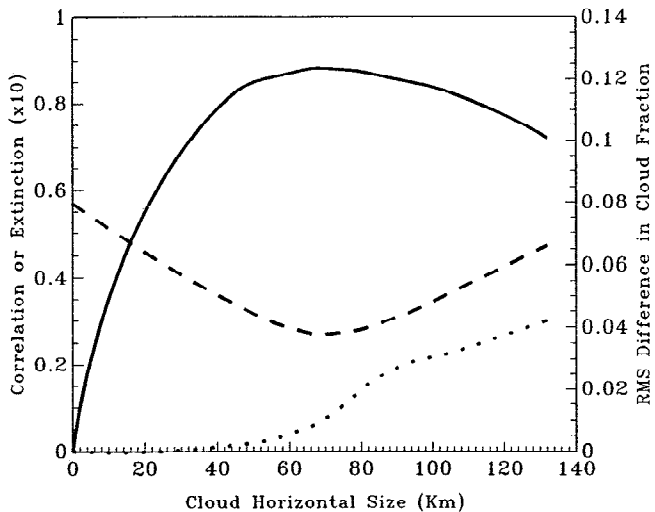
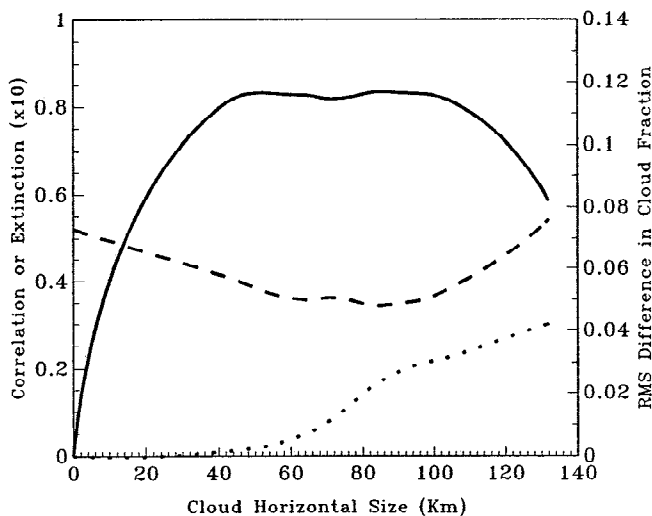


Figure 6. Scaling factor F/P_{cld} (see text) as a function of the effective horizontal dimension of clouds. The climatological cloud fraction is assumed to be 0.2 from ISCCP.



(a)



(b)

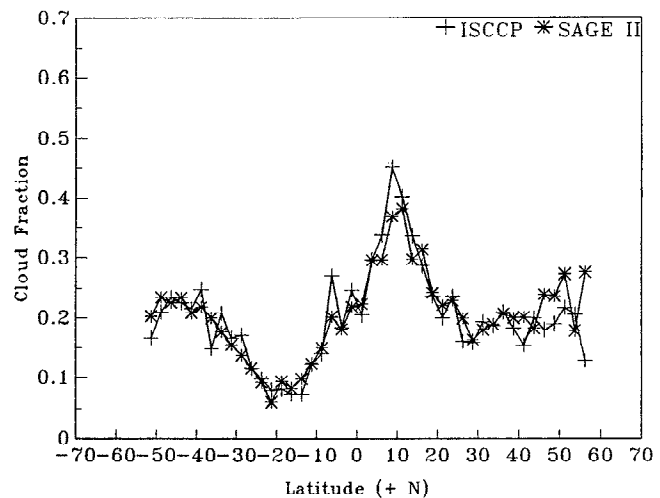
Figure 7. Variation of the correlation (solid line) and the rms differences between the monthly zonal mean SAGE II and ISCCP high-level cloud amounts (dashed line) obtained by using different combinations of threshold extinction coefficient, K (dotted line), and cloud horizontal sizes, l , in the analysis of SAGE II data for (a) July 1985–1990 and (b) January 1985–1990.

between 40 and 100 km and extinction thresholds between 0.001 and 0.025 km^{-1} produce the best match of the zonal mean SAGE II and ISCCP cloud fractions: The latitudinal correlation is >0.8 (significant at the 99.99% level), and the standard deviation of the differences $\delta = 0.04$. The optimum horizontal size from the July data sets is about 75 km with an extinction threshold of 0.008 km^{-1} . Figure 7b shows that the July parameters provide an equally good result for the January data sets. Figures 8a and 8b show the comparison of zonal mean high-level cloud amounts, and Table 2 gives the global mean results using these optimum parameters for SAGE II.

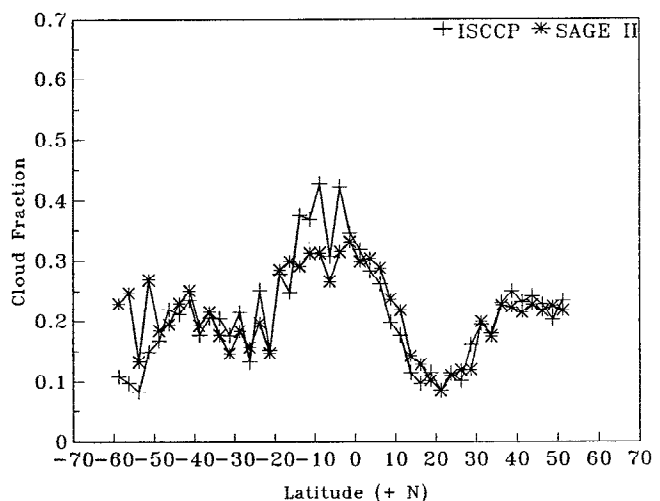
Two other studies have provided estimates of average cloud sizes. *Tian and Curry* [1989] present cloud amount frequency distributions for January 1979 over 40°N – 60°N from the United States Air Force

Three-Dimensional Nephelometry (3DNEPH) at horizontal resolutions of 45, 90, 221, and 445 km^2 . We calculated an average cloud size (one-dimensional only) from these distributions of about 73 km, where all clouds greater than 200 km are assumed to be 200 km. *Rossow et al.* [1993] show cloud amount frequency distributions for January 1984, July 1985 and October 1986 from ISCCP results and from surface observer reports. The estimated average cloud size from these two distributions is about 70–90 km. Thus these two studies imply an average cloud size similar to that which produces the best agreement between SAGE II and ISCCP high-level cloud amounts.

The optimum extinction threshold, 0.008 km^{-1} , is the same as that used by the SAGE team for the thicker “cirrus” clouds [Woodbury and McCormick, 1986], suggesting that both SAGE II and ISCCP capture essentially the same clouds at this threshold (excluding thinner clouds with $0.008 \text{ km}^{-1} < k < 0.0008 \text{ km}^{-1}$). This



(a)



(b)

Figure 8. Zonal mean high-level cloud fractions from ISCCP (lines with pluses) compared with SAGE II cloud fractions (lines with asterisks) using threshold extinction coefficients, $K=0.008 \text{ km}^{-1}$, and horizontal size $l = 75 \text{ km}$ (a) for July 1985–1990, and (b) for January 1985–1990.

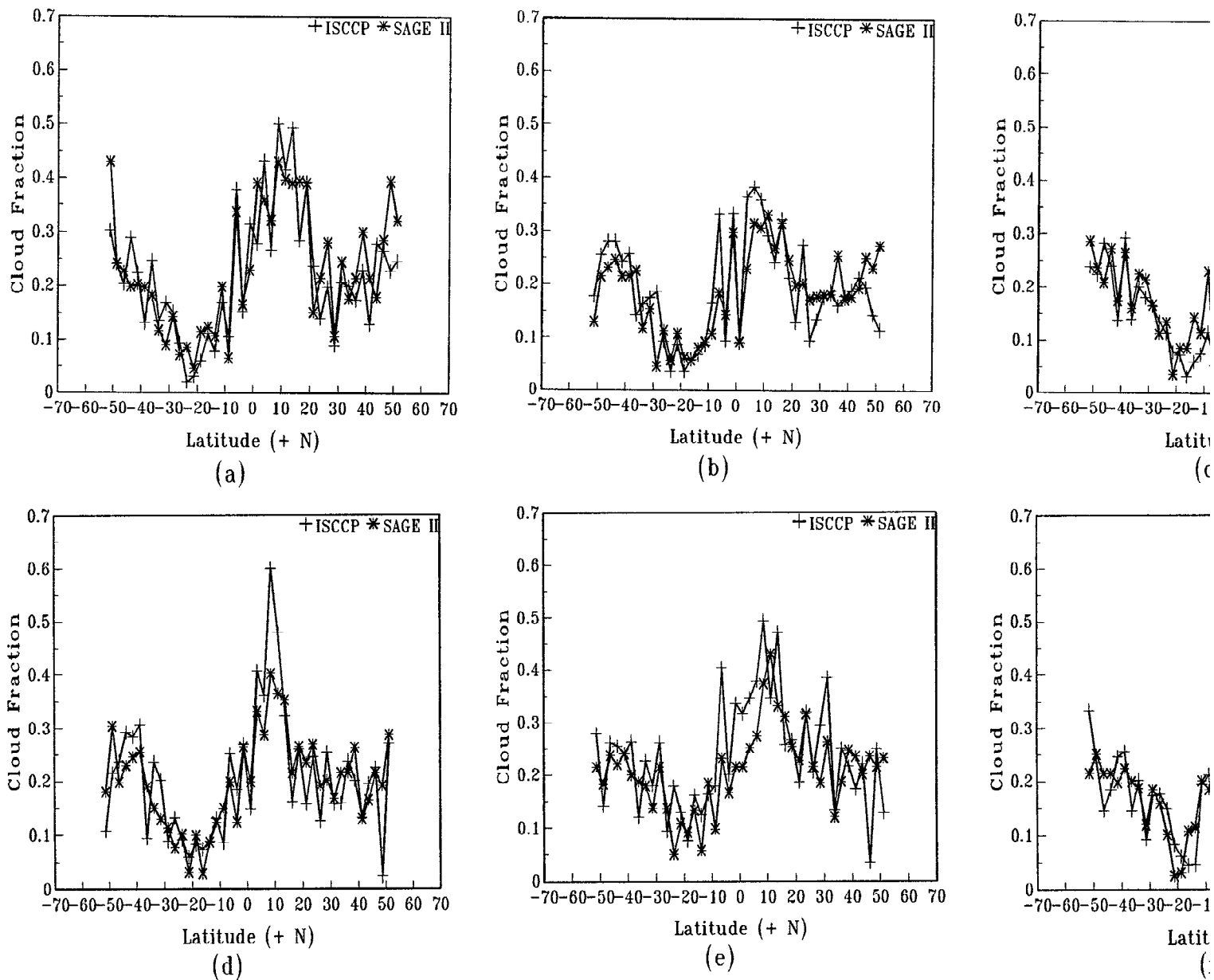


Figure 9. Monthly zonal mean high-level cloud fractions from SAGE II ($K = 0.008 \text{ km}^{-1}$ and $l = 75 \text{ km}$, lines with asterisks) and ISCCP (lines with pluses) for (a) July 1985, (b) July 1986, (c) July 1987, (d) July 1988, (e) July 1989, and (f) July 1990.

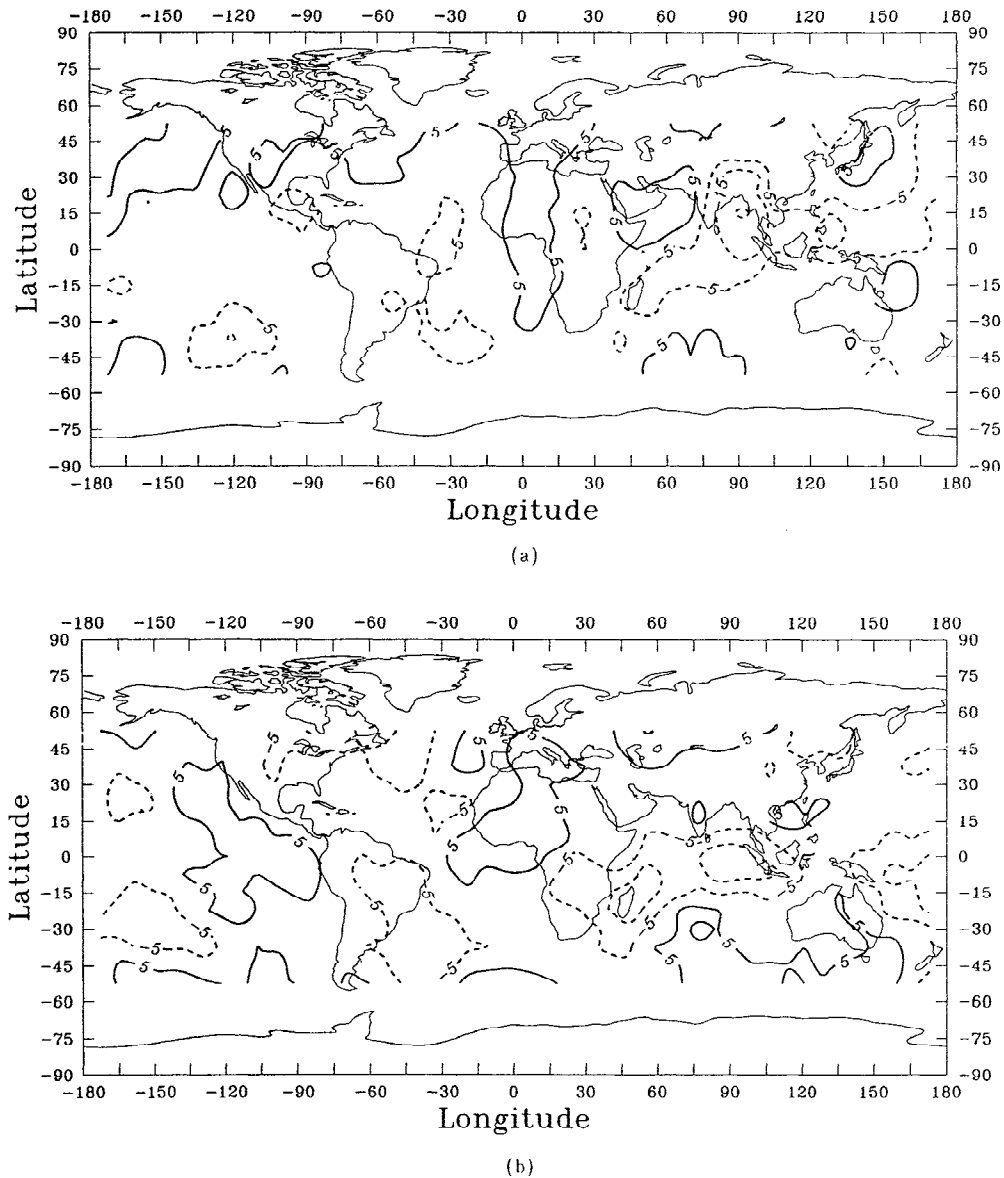


Figure 10. Geographical distribution of differences between SAGE II (using $K = 0.008 \text{ km}^{-1}$ and $l = 75 \text{ km}$) and ISCCP monthly mean cloud fractions for (a) July 1985–1990 and (b) January 1985–1990. Solid contours indicate that SAGE II cloud fractions are larger than ISCCP cloud fractions; dashed contours indicate that SAGE II values are less than ISCCP values. Contour intervals are 0.05, indicated by whole numbers.

is also roughly consistent with the estimated ISCCP detection limit when account is taken of the smaller average cloud size. Using equations (1) and (2), we find that the ISCCP detection limit, $\tau > 0.1\text{--}0.3$, is roughly equivalent to this extinction threshold if the vertical dimensions of high-level clouds are assumed to be at least 3 km and horizontal size is 75 km. It must be emphasized that this extinction threshold is optimum for the global average and may vary from region to region (see next section). However, the SAGE II analysis does detect much thinner clouds which ISCCP does not capture (see discussion in section 5.1).

Figure 7 shows clearly that although the best match of SAGE II and ISCCP is produced with an average cloud size, $l = 75 \text{ km}$, and an extinction threshold, $K = 0.008 \text{ km}^{-1}$, there is actually a range of these parameters that produces equivalent results. Varying cloud sizes over the range 40–100 km and extinction thresholds over the

range 0.001–0.025 km^{-1} does not alter the good agreement significantly. Thus many combinations of extinction and cloud horizontal size are possible, reflecting the actual complexity and the probable regional variability of cloud size distributions and optical thickness variations. The agreement between SAGE II and ISCCP for individual months (Figure 9) shows some year-to-year variability, particularly in the tropics, that could reflect variations in the effective cloud properties.

3.4. Geographical Distribution of SAGE II and ISCCP High Clouds

Although we found a single average cloud size and extinction coefficient that produces excellent agreement between global and zonal mean SAGE II and ISCCP high-level cloud amounts, this

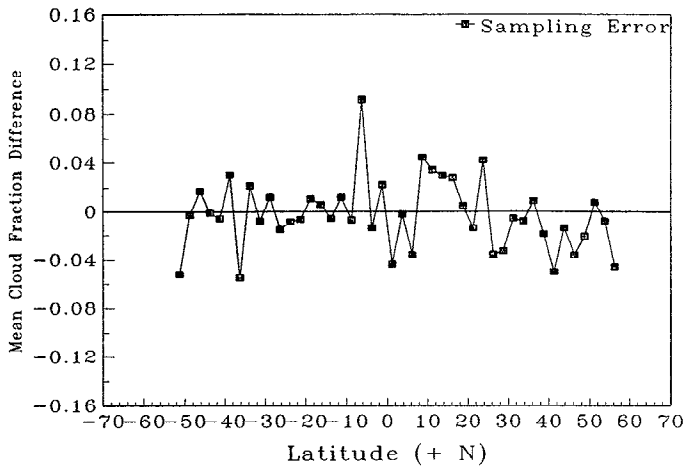


Figure 11. Mean difference in zonal mean cloud fraction, averaged over July 1985–1990, obtained from full ISCCP data and ISCCP sampled like SAGE II.

treatment neglects possible variations of average size with location and time. Figure 9 shows evidence for time variations. Examination of the geographical distribution of differences between the adjusted SAGE II and ISCCP high-level cloud amounts (Figure 10) indicates regions where the 75 km scale may be biased. Note that Figures 10a and 10b are smoothed over (8° latitude by 10° longitude) to filter out smaller-scale variations for clarity. In July (Figure 10a) there are notable negative differences (SAGE II cloud amount less than ISCCP cloud amount) of high-level cloudiness over the Indian monsoon region and African monsoon region, and positive differences (SAGE II cloud amount greater than ISCCP cloud amount) over the Sahara and Arabian regions (cf. Figure 15). The largest difference is over the Bay of Bengal, where other studies have shown that a significant fraction of the high-level clouds in these areas appear as mesoscale clusters with average radii of >100 km [e.g., Machado and Rossow, 1993]. This could explain why SAGE II

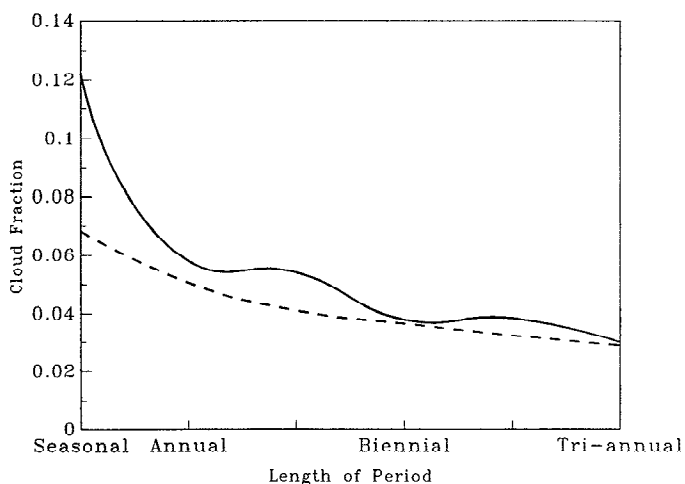


Figure 12. Root-mean-square differences between full ISCCP cloud fractions and those obtained from ISCCP sampled like SAGE II for 2.5° latitudinal bands (dashed line), and the rms variability in mean cloud fractions (solid line) from full ISCCP for averaging time periods of seasonal, annual, biennial, and triannual.

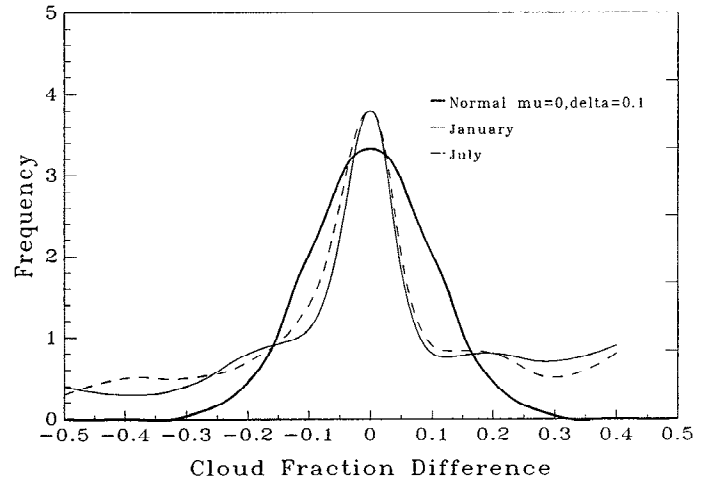


Figure 13. Frequency distribution of the differences between SAGE II and ISCCP mean cloud fractions for individual map grid boxes for July (thin solid line) and January (dashed line) 1985–1990. The thick solid line is a best fit Gaussian distribution with a mean, $\mu = 0$, and standard deviation, $\delta = 0.1$.

cloud amounts adjusted with a cloud horizontal size of 75 km are too low over these regions. Over the Sahara and Arabian cloud amount minima, SAGE II overestimates the cloud amounts, suggesting that clouds there may be less than 75 km in average horizontal size. A similar but smaller effect is also apparent over middle-latitude storm track regions. In January the tropical minima in high-level cloud amount differences shift to the other hemisphere; the adjusted SAGE II results are notably lower than the ISCCP over Brazil and Indian Ocean but still higher over the Sahara cloud minima (Figure 10b). The changes in location of the tropical negative difference regimes follow the climatological locations of the most active convection as expected.

Although the geographical variations of cloud amount differences between SAGE II and ISCCP clouds mentioned above can be explained solely by plausible variations of cloud horizontal extent, it is also possible that some variations in Figure 10 are associated with changes in the optimum SAGE II cloud detection optical threshold above the constant value we used. It is also possible that both cloud size and threshold vary with location and season. However, it is difficult to estimate a location-dependent SAGE II cloud detection threshold because we do not have enough information to separate threshold effects from variations in the horizontal extent of clouds. However, since SAGE II cloud amounts are much more sensitive to the cloud horizontal size we use than the detection threshold we choose, we favor the interpretation for geographical variations given above.

4. Errors and Uncertainties

4.1. Uncertainties in SAGE II Zonal Climatological Averages

We can test the effects of SAGE II sampling on its zonal average cloud amounts by comparing the original ISCCP C1 data set with the ISCCP data set matched to SAGE II (called “sampled ISCCP”). Figure 11 shows the differences in zonal mean cloud amounts for July 1985–1992. SAGE II sampling errors are about 0.04. For illustration, July and January are used to represent different seasons, and the averages over July and January are used to represent annual

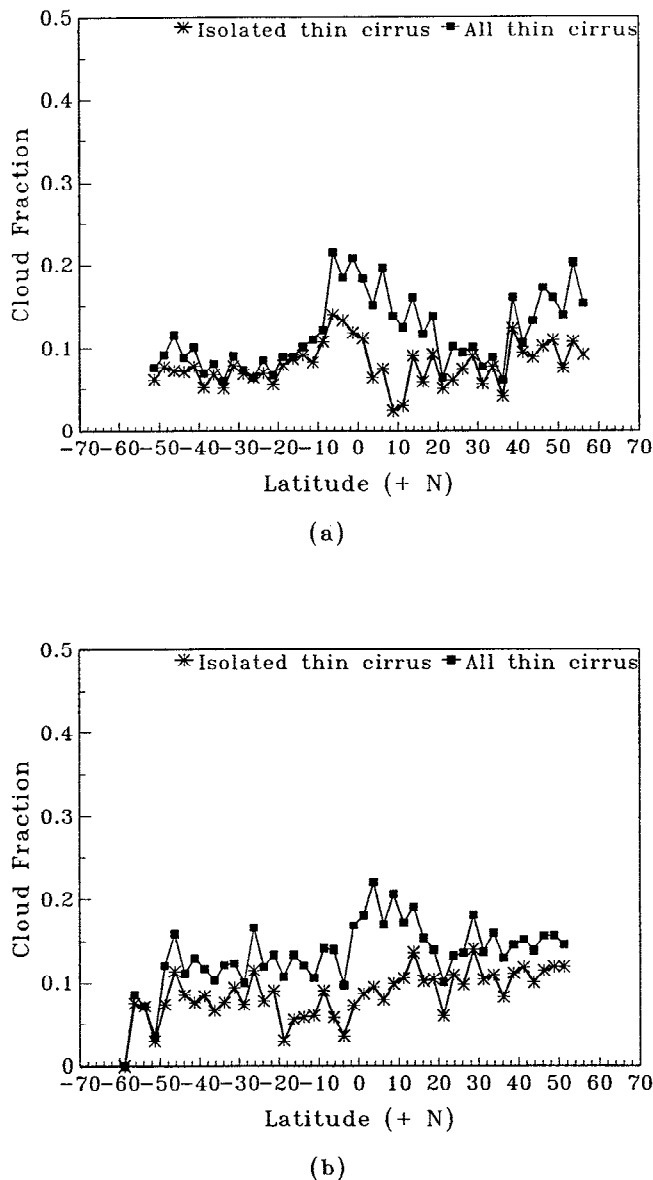


Figure 14. Monthly zonal mean thin cirrus cloud fractions, defined by extinction coefficients, $0.0008 \text{ km}^{-1} < k_i < 0.008 \text{ km}^{-1}$, and cloud horizontal size, $l = 75 \text{ km}$, for (a) July 1985–1990 and (b) January 1985–1990. The lines with asterisks show the amount of thin cirrus clouds with no other high-level clouds below them; the line with squares indicates the total amount of thin cirrus clouds including those with other high-level clouds below.

means to calculate seasonal, annual, biennial, and triennial variabilities from 6 years of data. For each time scale and each latitudinal band, the rms differences between the average values from ISCCP and sampled ISCCP are calculated and compared with the rms time variations of the averages from ISCCP. For example, the rms differences between monthly mean values from ISCCP and sampled ISCCP are compared to the rms month-to-month variations of the ISCCP cloud amounts. The results are summarized in Figure 12 by showing the rms of results from all latitudinal bands. As the averaging period increases (sample population increases), the rms difference between averages for 2.5° latitudinal bands from ISCCP

and sampled ISCCP decreases. The differences, interpreted as sampling errors for SAGE II results, are smaller than the seasonal variability measured by ISCCP but comparable to the observed interannual variations. No bias errors are found with the SAGE II sampling.

To investigate the sensitivity of this result on the resolution chosen, we also calculated the rms differences for larger regions (10°) and found that the SAGE II sampling errors are reduced by about half. However, the full ISCCP averaged over the 10° latitudinal bands also exhibits the same reduction in the natural variability. Thus SAGE II data can monitor seasonal variations down to latitudinal zones of a few hundred kilometers, but they cannot monitor interannual variability due to the large error in sampling the natural variations.

4.2. Errors Due to the Choice of Cloud Horizontal Size

We found much better agreement in high-level cloud amounts between SAGE II and ISCCP by assuming that the average cloud horizontal dimension is $l = 75 \text{ km}$. Differences between this value of l and the actual cloud dimensions and distribution along the 200 km path introduce uncertainty in individual SAGE II values. If the variations of average cloud sizes with location are random, we would expect a Gaussian distribution of the differences between individual SAGE II and ISCCP values with a mean value, μ , and a standard deviation, σ . Figure 13 compares the frequency distribution of these differences from July and January data with a best fit normal distribution. The general shape is close to a Gaussian distribution with $\mu \approx 0$ and $\sigma = 0.10$; however, the “tails” at larger differences indicate that about 15% of the cases exhibit much larger differences between SAGE II and ISCCP cloud amounts than are larger than expected. Correlating the larger differences with the mean ISCCP cloud fraction shows that the large positive differences are associated with very low ISCCP cloud amounts, whereas the large negative differences are associated with very high ISCCP cloud amounts. Figure 10 shows the geographic locations of these two populations: the large positive difference cases are in regions of scattered cloudiness, while the large negative difference cases are in regions of persistent large convective complexes. A best fit Gaussian, excluding the two extreme groups gives $\sigma = 0.06$; i.e., the random uncertainty in monthly mean SAGE II cloud amounts is about this amount, except in the regions highlighted in Figure 10 where the uncertainty is about two to three times larger.

5. Discussion and Summary

5.1. Very Thin Cirrus

Woodbury and McCormick [1986] defined “thin cirrus” in the SAGE II data by extinction coefficients $0.0008 \geq k_i > 0.008 \text{ km}^{-1}$. For a cloud with typical horizontal size of 75 km and the vertical extent of of 2.5 km [see Liao *et al.*, this issue], such a cloud would have τ between 0.005 and 0.05, below the detection limit for ISCCP. However, a deeper cloud layer might be marginally detected by ISCCP. Nevertheless, the best match between SAGE II and ISCCP required a reduction in the SAGE II detection sensitivity (k_i from 0.0008 to 0.008 km^{-1}) implying that ISCCP is not able to detect these optically thinner clouds ($0.0008 \text{ km}^{-1} < k_i < 0.008 \text{ km}^{-1}$), observed by SAGE II. Assuming the same average horizontal cloud size of 75 km, we determine the zonal mean thin cirrus amounts for July and January 1985–1990 (Figure 14). The global mean thin cirrus amount is about 0.09 for clouds that do not have any other high-level cloud below them (called isolated thin cirrus); however,

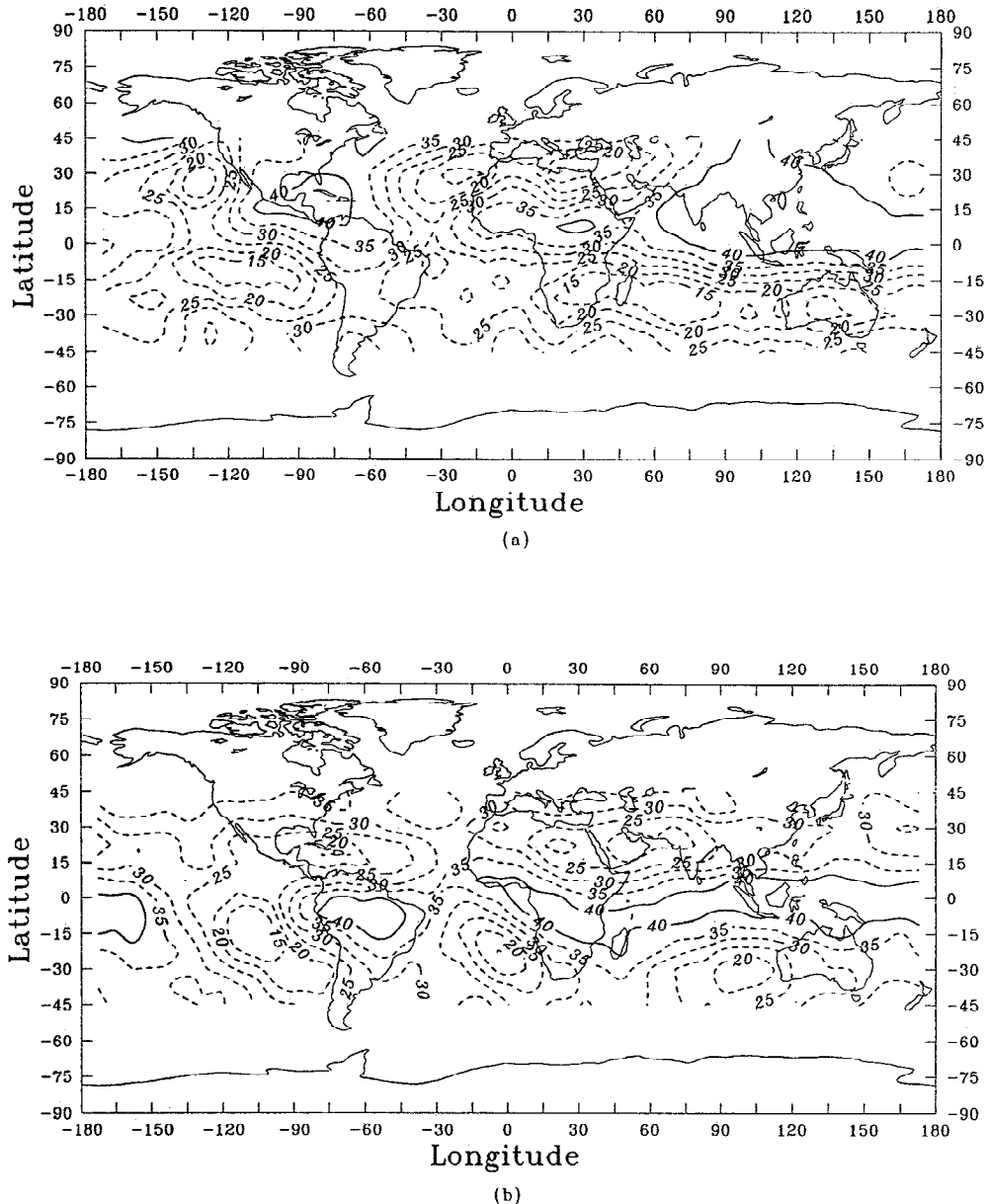


Figure 15. Mean global distribution of all high-level clouds from SAGE II, using $K = 0.0008 \text{ km}^{-1}$ and $l = 75 \text{ km}$, for (a) July 1985–1990 and (b) January 1985–1990. Contour interval is 0.05 from 0.10 to 0.40, shown as whole numbers.

there is another 0.03 of thin cirrus layers that are found overlying thicker ($k > 0.008 \text{ km}^{-1}$) high-level cloud tops, mostly in the tropics. Isolated thin cirrus appear to be evenly distributed with latitude, but there is a small decrease of such clouds in the vicinity of the ITCZ where more thin clouds occur above thicker clouds. SAGE II suggests a total high-level cloud amount of about 0.30 (0.21 ISCCP matched plus 0.09 ISCCP not matched) in contrast with the ISCCP value of 0.21.

5.2. What Is the Distribution of High-Level Clouds?

Figure 15 shows the geographic distribution of all high-level clouds from SAGE II ($K = 0.0008 \text{ km}^{-1}$ and $l = 75 \text{ km}$), averaged

over six Julys and six Januaries (Table 3 provides a summary). The most notable features are the tropical concentrations of high-level clouds (>0.40) associated with concentrations of deep convection over Central America and southeast Asia in July and over Brazil, central Africa, and Indonesia in January [cf. Machado and Rossow, 1993]. The SAGE II values probably underestimate the peak cloud amounts in these areas because using a value of $l = 75 \text{ km}$ limits the maximum cloud amount to about 0.43. Notable minima of high-level cloudiness (<0.20) occur over the subtropical regions with persistent marine stratocumulus clouds located off the west coasts of the continents. These minima may be slightly overestimated by SAGE II because cloud size in these regions may be smaller than 75 km. Figure 16 highlights the lack of contrast in the average

Table 3. Summary of High-Level Cloud Amounts From SAGE II for July and January, Averaged Over 1985–1990

	Over All Regions		Over Sea		Over Land	
	July	January	July	January	July	January
Globe	0.297	0.316	0.296	0.302	0.314	0.323
Northern Hemisphere	0.343	0.312	0.317	0.317	0.356	0.303
Southern Hemisphere	0.247	0.317	0.250	0.310	0.237	0.336
ISCCP (Globe)	0.203	0.218	0.201	0.215	0.210	0.221

Extinction 0.0008 km^{-1} and an optimum effective cloud horizontal size of 75 km are used extinction 0.0008 km^{-1} and the optimum effective cloud horizontal size of 75 km.

cloud amounts over ocean and land. This figure also shows that seasonal variations are associated with shifting locations of the ITCZ and the midlatitude storm tracks, particularly in the northern hemisphere.

5.3. Summary

The following are the main conclusions of this paper:

1. Zonal monthly mean high-level cloud amounts derived from SAGE II and ISCCP agree well if an extinction threshold of 0.008 km^{-1} and an effective cloud horizontal dimension of 75 km are assumed in the SAGE II analysis. It is remarkable that only two parameters produce such good agreement between the SAGE II and ISCCP high-level cloud amounts. One implication is that high-level clouds that are undetectable by ISCCP are not the dominant high-level cloud type. However, there are important regional discrepancies that suggest locations where the average effective cloud dimension is either smaller or larger than 75 km, most notably

areas dominated by mesoscale convective complexes which apparently have an average size of $>100 \text{ km}$.

2. SAGE II indicates the presence of about 0.12 very thin cirrus (extinction coefficient between 0.0008 and 0.008 km^{-1}), about 0.03 of which overlays other high-level clouds. The latitudinal distribution of these clouds is nearly uniform. About one third of high-level cloud is missed by ISCCP, but the estimated optical thicknesses of these clouds (assuming vertical and horizontal dimensions of 2.5 km and 75 km) is <0.1 .

3. SAGE II sampling errors in the zonal mean cloud fraction are smaller than the observed seasonal variations indicated by the ISCCP data; however, SAGE II sampling errors are comparable with the interannual variability indicated by ISCCP data.

The general agreement between the SAGE II and ISCCP data sets allows us to use SAGE II to investigate the vertical structure of the uppermost portions of clouds [Liao *et al.*, this issue]. The results are important for understanding high-level clouds and for verifying the determinations of cloud top heights from ISCCP.

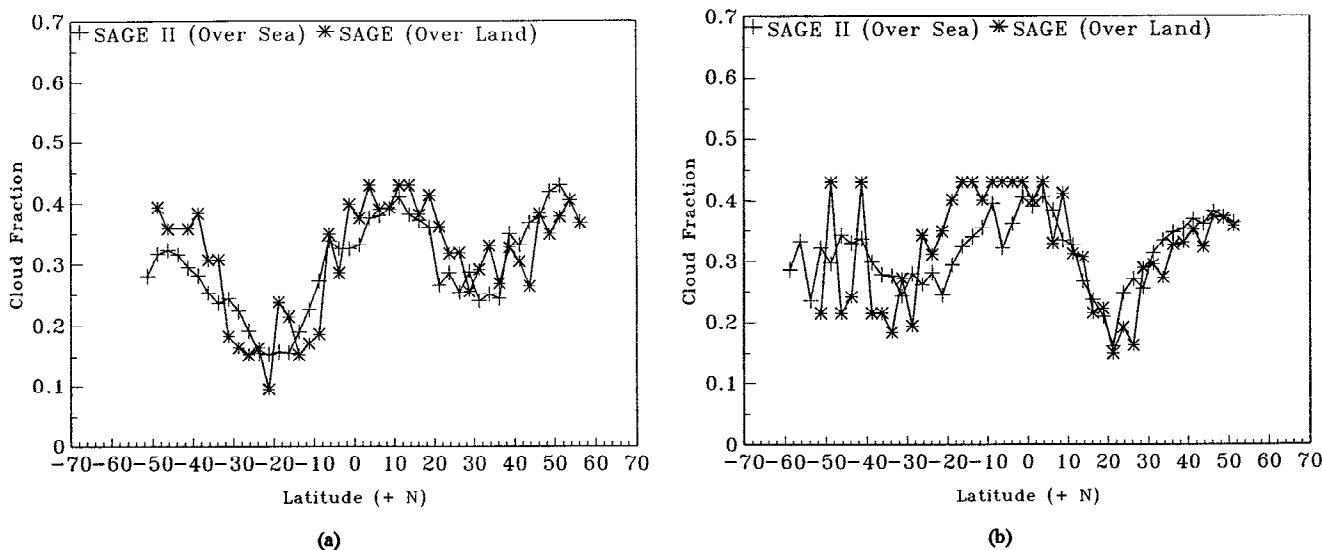


Figure 16. Monthly zonal mean high-level cloud fractions from SAGE II, using $K = 0.0008 \text{ km}^{-1}$ and $l = 75 \text{ km}$, averaged over ocean (lines with pluses) and over land (lines with asterisks) for (a) July 1985–1990 and (b) January 1985–1990.

Acknowledgements. SAGE II data and technical information were provided by the SAGE II science team at the NASA Langley Research Center. Special thanks to W. P. Chu for discussion of saturated profiles. A. Walker and J. Lerner provided programming help to access the satellite data sets. Reto Ruedy provided general programming assistance. This work was supported by the NASA SAGE II Science Program and the Department of Energy.

References

- Barton, I. J., Upper level of cloud climatology from an orbiting satellite, *J. Atmos. Sci.*, **40**, 435-447, 1983.
- Cahalan, R. F., and J. H. Joseph, Fractal statistics of clouds, *Mon. Weather Rev.*, **117**, 261-272, 1989.
- Chu, W. P., and M. P. McCormick, Inversion of stratospheric aerosol and gaseous constituents from spacecraft solar extinction data in the 0.38-1.0 μm wavelength region, *Appl. Opt.*, **18**, 1404-1413, 1979.
- Chu, W. P., E. W. Chiou, J. C. Larsen, L. W. Thomason, D. Rind, J. J. Buglia, S. Oltmans, M. P. McCormick, and L. M. McMaster, Algorithms and sensitivity analyses for Stratospheric Aerosol and Gas Experiment II water vapor retrieval, *J. Geophys. Res.*, **98**, 4857-4866, 1993.
- Dowling, D. R., and L. F. Radke, A summary of the physical properties of cirrus clouds, *J. Appl. Meteorol.*, **29**, 970-970, 1990.
- Jones, P. A., Cloud-cover distributions and correlation, *J. Appl. Meteorol.*, **31**, 732-741, 1992.
- Kent, G. S., D. M. Winker, M. T. Osborn, and K. M. Skeens, A model for the separation of cloud and aerosol in SAGE II occultation data, *J. Geophys. Res.*, **98**, 20,725-20,735, 1993.
- Liao, X., W. B. Rossow, and D. Rind, Comparison between SAGE II and ISCCP high-level clouds, 2, Locating cloud tops, *J. Geophys. Res.*, this issue.
- Machado, L. A. T., and W. B. Rossow, Structural characteristics and radiative properties of tropical cloud clusters, *Mon. Weather Rev.*, **21**, 3234-3260, 1993.
- McCormick, M. P., Initial assessment of the stratospheric climatic impact of the 1991 Mount Pinatubo eruption: Prologue, *Geophys. Res. Lett.*, **19**, 149, 1992.
- McCormick, M. P., H. B. Edwards, L. E. Maudin III, and L. R. McMaster, *Atmospheric aerosols: Their optical properties and effects*, NASA Rep. CP2004, p. TUB2, 1976.
- McCormick, M. P., P. Hamill, T. J. Pejin, W. P. Chu, T. J. Swissler, and L. R. McMaster, Satellite studies of the stratospheric aerosol, *Bull. Am. Meteorol. Soc.*, **60**, 1038-1045, 1979.
- Ramaswamy, V., and V. Ramanathan, Solar absorption by cirrus clouds and the maintenance of the tropical upper troposphere thermal structure, *J. Atmos. Sci.*, **46**, 2293-2310, 1989.
- Randall, D. A., Harshvardhan, D. A. Dazlich, and T. C. Corsetti, Interactions among radiation, convection and large-scale dynamics in a general circulation model. *J. Atmos. Sci.*, **46**, 1943-1970, 1989.
- Rind, D., E. W. Chiou, W. Chu, S. Oltmans, J. Learner, J. Larsen, M. P. McCormick, and L. McMaster, Overview of the Stratospheric Aerosol and Gas Experiment II water vapor observations: Method, validation and data characteristics, *J. Geophys. Res.*, **98**, 4835-4856, 1993.
- Rossow, W. B., and L. C. Garder, Cloud detection using satellite measurements of infrared and visible radiances for ISCCP, *J. Clim.*, **6**, 2341-2369, 1993a.
- Rossow, W. B., and L. C. Garder, Validation of ISCCP cloud detections, *J. Clim.*, **6**, 2370-2393, 1993b.
- Rossow, W. B., and R. A. Schiffer, ISCCP cloud data products, *Bull. Am. Meteorol. Soc.*, **72**, 2-20, 1991.
- Rossow, W. B., L. G. Garder, P. Lu, and A. W. Walker, International Satellite Cloud Climatology Project (ISCCP) Documentation of cloud data, *Tech. Doc. WMO/TD 266 (revised)*, 76 pp, World Meteorol. Org., Geneva, 1991.
- Rossow, W. B., A. W. Walker, and L. C. Garder, Comparison of ISCCP and other cloud amounts, *J. Clim.*, **6**, 2394-2418, 1993.
- Schiffer, R. A., and W. B. Rossow, The International Satellite Cloud Climatology Project (ISCCP): The first project of the World Climate Research Program, *Bull. Am. Meteorol. Soc.*, **64**, 779-784, 1983.
- Seze, G., and W. B. Rossow, Effect of satellite data resolution on measuring the space-time variations of surface and clouds, *Int. J. Remote Sens.*, **12**, 921-952, 1991.
- Slingo, A., and J. M. Slingo, The response of a general circulation model to cloud longwave radiative forcing, I, Introduction and initial experiment. *Q. J. R. Meteorol. Soc.*, **114**, 1027-1062, 1988.
- Tian, L., and J. A. Curry, Cloud overlap statistics, *J. Geophys. Res.*, **94**, 9925-9935, 1989.
- Warren, S. G., C. J. Hahn, and J. London, Simultaneous occurrence of different types, *J. Appl. Meteorol.*, **24**, 658-667, 1985.
- Welch, R. M., K. S. Kuo, B. A., Wielicki, S. K. Sengupta, and L. Parker, Marine stratocumulus cloud fields off the coast of southern California observed using LANDSAT imagery, I, Structural characteristics, *J. Appl. Meteorol.*, **27**, 341-362, 1988.
- Wielicki, B. A., and L. Parker, On the determination of cloud cover from satellite sensors: The effect of sensors on spatial resolution, *J. Geophys. Res.*, **97**, 12,799-12,823, 1992.
- Woodbury, G. E., and M. P. McCormick, Zonal and Geographical distribution of cirrus clouds determined from SAGE II data, *J. Geophys. Res.*, **91**, 2775-2785, 1986.

X. Liao, D. Rind, and W. B. Rossow, NASA Goddard Institute for Space Studies, 2880 Broadway, New York, NY 10025. (email: cdxxl@nasagiss.giss.nasa.gov)

(Received October 20, 1993; revised August 24, 1994; accepted September 16, 1994.)